

# REVISIT OF NONLINEAR DYNAMICS IN HÉNON MAP USING SQUARE MATRIX METHOD\*

Yue Hao<sup>†</sup>, K. Anderson, Michigan State University, East Lansing, MI, USA  
Li-Hua Yu, Brookhaven National Laboratory, Upton, NY, USA

## Abstract

Hénon map represents a thin lens sextupole in an otherwise linear lattice and had been well studied for many decades. We revisit the Hénon map with an iteration procedure to transform nonlinear perturbed trajectory to a rigid rotation, followed by KAM theory. The convergence of the iteration is determined by the resonance structure. With the aid of the square matrix method, we will demonstrate that the iteration procedure is powerful in calculating the amplitude-tune dependence and the area of the central stable region of the Hénon map.

## HÉNON MAP

Hénon map, specifically its area preserve case, has the following form:

$$\begin{pmatrix} x \\ p \end{pmatrix}_{n+1} = \begin{pmatrix} \cos \mu & \sin \mu \\ -\sin \mu & \cos \mu \end{pmatrix} \begin{pmatrix} x \\ p - x^2 \end{pmatrix}_n. \quad (1)$$

It describes the 1-D dynamics of a thin sextupole in a other-wise simple rotation lattice.

To diagonalize the linear matrix, we can rewrite it using complex variable  $z = x - ip$  and Hénon map becomes:

$$z_{n+1} = z_n e^{i\mu} + \frac{i}{4} (z_n + z_n^*)^2 e^{i\mu}. \quad (2)$$

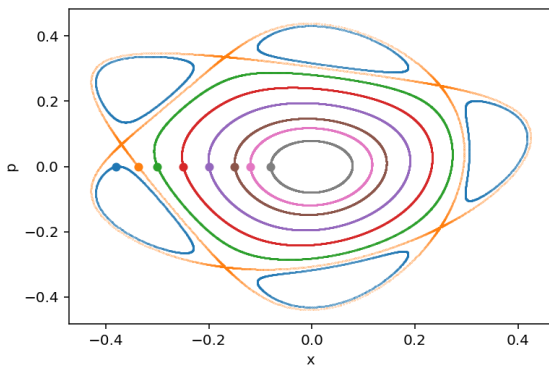


Figure 1: The phase space contour of Hénon map with linear tune 0.205. The dots represents the initial condition of each trajectory.

The phase space trajectory is shown in Fig. 1 when the linear tune is 0.205. The initial values are chosen on the

\* Work supported by Accelerator Stewardship program under award number DE-SC0019403.

<sup>†</sup> haoyue@msu.edu

negative x axis. The major resonance is the 5<sup>th</sup> resonance which forms 5 islands, separated from the central island by a separatrix passing  $x_s \approx -0.33732$ .

In this article, we are demonstrating a method that transforms the trajectory within the central island to a rigid rotation.

## RIGID ROTATION

According to KAM theory [1], some of the invariant tori survive under small nonlinear perturbation, when the frequency is sufficiently irrational (Diophantine condition). In this section, we will examine the phase space region where such invariant tori survive, which is characterized by whether diffeomorphism to a rigid rotation at specific initial conditions can be found.

In the Hénon map, if the trajectory of the map  $(z_0, z_1, \dots, z_n, \dots)$  is a bounded and pseudo-periodic motion, it is more convenient to express the complex coordinate  $z$  in terms of a complex phase:  $z = e^{i\theta}$ . The Hénon Map comes:

$$\theta_{n+1} = \theta_n + \mu - i \log \left( 1 + \frac{ie^{-i\theta_n}}{4} (e^{i\theta_n} + e^{-i\theta_n}^*)^2 \right) \quad (3)$$

$$= \theta_n + f(\theta_n, \theta_n^*), \quad (4)$$

here,  $\theta$  has real part representing the argument of  $z$  and imaginary part which is the logarithm of the amplitude. If the trajectory  $(\theta_0, \theta_1, \theta_2, \dots, \theta_n, \dots)$  is a pseudo-periodic one, we expect to find a diffeomorphism to a rigid rotation:

$$\theta = \alpha + h(\alpha), \quad (5)$$

where  $h$  is a periodic and smooth complex function, with period of  $2\pi$ , i.e.  $h(\alpha) = h(\alpha + 2\pi)$ , and  $\alpha$  is the angle of a pure rigid rotation:

$$\alpha_{n+1} = \alpha_n + \rho, \quad (6)$$

here  $\rho$  is the rotation number of the trajectory,

$$\rho = \lim_{n \rightarrow \infty} \frac{\theta_n - \theta_0}{n}. \quad (7)$$

As a periodic function,  $h$  can be expressed as a Fourier series.

$$h = \sum_{m=-\infty}^{\infty} h_m e^{ima}. \quad (8)$$

To solve the rotation number and the diffeomorphism, a direct way is to use the iterations on the map, starting from the preset initial value ( $z_0 = x_0 - ip_0$ ). When inserting Eq. (5) in Eq. (4), we have

$$h(\alpha + \rho) - h(\alpha) = f(\alpha + h(\alpha), \alpha + h^*(\alpha)) - \rho. \quad (9)$$

For simplicity, we will rename the right hand side of above equation as  $\eta(\alpha; h, \rho)$  below.

Equation (9) can be solved iteratively, with the constrain that the trajectory always passes through a fix point  $\theta_0$ . The simplest initial condition is  $h^{(0)} = \theta_0 - \alpha_0$ , which is the good approximated solution in the vicinity of  $z = 0$ . In each iteration, we are solving:

$$h^{(n+1)}(\alpha + \rho^{(n+1)}) - h^{(n+1)}(\alpha) = \eta(\alpha; h^{(n)}, \rho^{(n+1)}),$$

where the subscripts denotes the number of iterations. The  $(n+1)^{\text{th}}$  iteration should be done in three steps. First, the left-hand side always have vanished zeroth Fourier component. Therefore, it requires the zeroth Fourier component of the right hand side also vanish, which implies the constrain for the only free parameter  $\rho^{(n+1)}$ .

$$\int_0^{2\pi} \eta(\alpha; h^{(n)}, \rho^{(n+1)}) d\alpha = 0. \quad (10)$$

Second, the  $m^{\text{th}}$  ( $m \neq 0$ ) Fourier component of  $h$  of  $(n+1)^{\text{th}}$  iteration,  $\hat{h}_m^{(n+1)}$ , can be written as

$$\hat{h}_m = \frac{\hat{\eta}_m^{(n)}}{e^{im\rho^{(n+1)}} - 1}, \quad (11)$$

where  $\hat{\eta}_m^{(n)}$  is the  $m^{\text{th}}$  component of  $h$  of  $n^{\text{th}}$  iteration, which read:

$$\hat{\eta}_m^{(n)} = \int_0^{2\pi} \eta(\alpha; h^{(n)}, \rho^{(n+1)}) e^{-ima} d\alpha. \quad (12)$$

Equation (11) is valid only if the Fourier expansion of  $h$  is valid, i.e.  $e^{im\rho_{n+1}} \neq 1$ .

At last, the average of  $h^{(n+1)}$  (zeroth order Fourier component  $\hat{h}_0^{(n+1)}$ ) is still unknown, we choose to set it by forcing the diffeomorphism stays on the initial value, i.e., existing a angle  $\alpha^*$  which satisfy

$$\theta_0 = \alpha^* + h^{(n+1)}(\alpha^*).$$

Through the above iterative steps, we can achieve both the frequency and trajectory of the Hénon map from a given initial condition, using numerical calculation. In the numerical evaluation, function  $\eta$  has to be represented by  $n_s$  discrete point of  $\alpha$  in  $[0, 2\pi)$ .  $n_s$  should be selected so that all important resonance can be resolved, whereas the  $n^{\text{th}}$  order needs  $n_s \geq 2n$  points. It is worthwhile to note that, when large  $n_s$  is adopted, the high order Fourier component will be small and its numerical results (in Eq. (12)) will be dominated by the numerical noise when Fourier transformation is performed and fail the iteration process. Therefore, in this case, we have to suppress the noise of those Fourier components following the idea of the Paley-Wiener Theorem.

Figure 2 indicates a successful iteration process for starting point at  $x = -0.3$  in Fig. 1. In this example,  $n_s = 64$  is chosen. The frequency reaches a saturated value 0.201921849, which only differs  $10^{-16}$  between iterations after initial 320 iterations. This is referred to as iteration accuracy later. The value is very close to the frequency determined from tracking, 0.201921837, which is calculated

using the NAFF algorithm [2] from 10M turns tracking results. The relative difference of the frequency is in order of  $10^{-8}$ , while the iterations process can be calculated using only a small portion of time (about 20 times less). It is worthwhile to note that the frequency difference is different from the iteration accuracy since the iteration process involves truncation in the Fourier series.

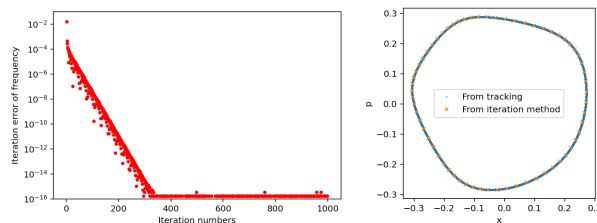


Figure 2: Iteration process for initial starting point  $(x,p)=(-0.3,0)$ . Left: The relative frequency difference between consecutive iterations; Right: Comparison of trajectory from tracking and the iterative process.

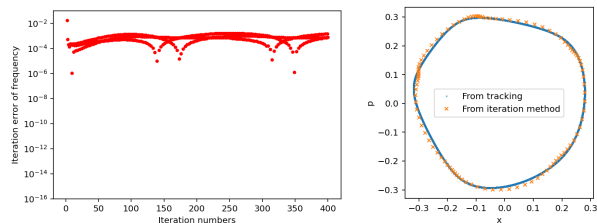


Figure 3: A failed example of the iteration process compared with Fig. 2. The initial starting point is  $(x,p)=(-0.31,0)$ .

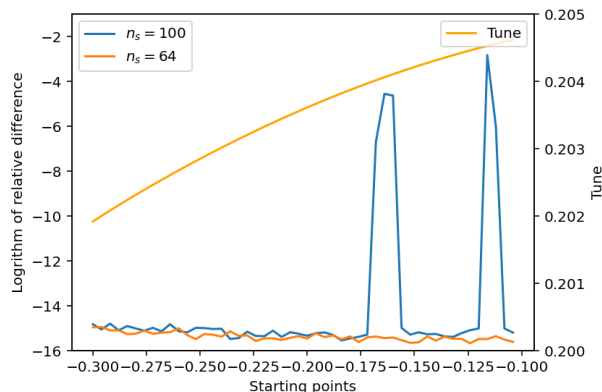


Figure 4: A failed example of the iteration process compared with Fig. 2. The initial starting point is  $(x,p)=(-0.31,0)$ .

When the initial value deviate from origin to some extent, the iteration process starts to break before reaching the major resonance. Figure 3 shows the process failed when slight pushing the starting point in outward direction, to 0.31. The iteration accuracy remains  $10^{-4}$  level during the entire iteration process. It is due to the function  $\eta(\alpha)$  is not smooth

enough, so that the derivative of the Fourier component of the resonance term is greater than one.

It is worthwhile to note that, there are many higher-order resonances in the central island of Hénon map. None of them has its order number lower than 40 in the range  $[0.2, 0.205]$ . Therefore they cannot be resolved with  $n_s = 64$ . In Fig. 4, we compared the iteration accuracy between using  $n_s = 64$  and  $n_s = 100$ , for different starting points from  $-0.1$  to  $-0.3$ . Two peaks are found in the iteration accuracy in the logarithm plot of  $n_s = 100$ , which is high enough to resolve resonances of  $10/49$  and  $9/44$  respectively.

## ADOPTING SQUARE MATRIX METHOD

The above iteration method failed to transform the phase space trajectory to a rigid rotation when approaching the separatrix of a major resonance. The Square Matrix Method (SMM) can be adopted to pre-transform it to a pseudo action-angle-pair to provide a more smooth function for this iteration process. The square matrix in SMM is constructed from the Hénon map. Followed SMM procedure, a truncated (at order  $N$ ) polynomial transformation can be found as

$$w = U(z, z^*, z^2, zz^*, z^{*2}, \dots), \quad (13)$$

while its inverse function, accurate up to order  $N$  can be found as:

$$z = U^{-1}(w, w^*, w^2, ww^*, w^{*2}, \dots), \quad (14)$$

where  $U$  is given by the generalized eigenvector from Jordan decomposition of the square matrix, and its approximated inverse function  $U^{-1}$  satisfies  $U^{-1} \circ U = I + \mathcal{O}(z^{N+1})$ . Since the study is close to 5<sup>th</sup> order resonance, the square matrix is constructed as a 'degenerate' case where the tune of the map is set to be exactly on resonance  $\mu = 0.2 \times 2\pi$ .

If the Hénon map using variable  $z$  has the form  $H(z)$ , the map is approximated to be

$$U \circ H \circ U^{-1}, \quad (15)$$

when the independent variable is changed to  $w$ . It is not an exact map because of the approximated inverse transformation due to truncation of the Taylor map. By redefining  $\theta = -i \log w$ , we can follow the treatments and iteration from Eq. (5) to Eq. (12) again and check the convergence when the initial value is closer to the separatrix.

First a low order (5<sup>th</sup> order) SMM is used on Hénon map. The upper two plots in Fig. 5 indicates that the iteration procedure now works on an initial condition,  $x_{ini} = -0.335$ , that is much closer to the separatrix ( $x_s \approx -0.337$ ), comparing with Fig. 3 which indicates the iteration stops convergence when  $x_{ini} \leq -0.31$ . However, there is a larger frequency discrepancy ( $10^{-4}$  level) compared with the particle tracking, when the 5<sup>th</sup> order SMM is used. We believe it is due to two reasons. First, the trajectory is not as smooth near the separatrix, therefore more sampling points have to be selected.

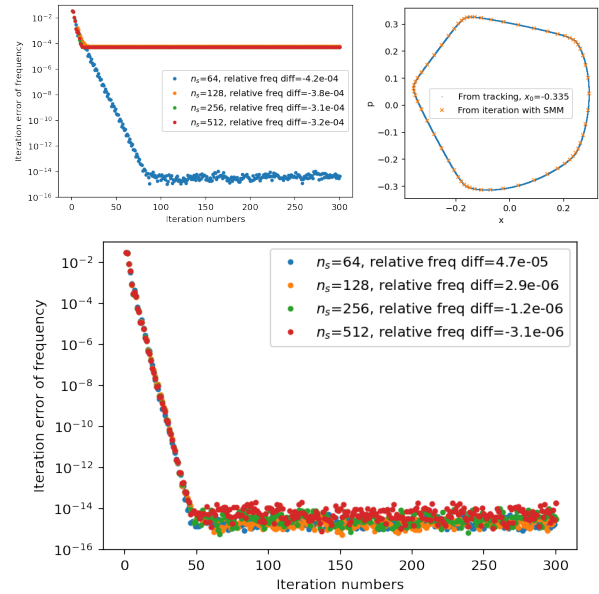


Figure 5: The iteration process based on transformation using SMM. The initial starting point is  $(x,p)=(-0.335,0)$ .

The top left plot in Fig. 5 shows a slight improvement when increasing  $n_s$  from 64 to 256. The second factor, which is dominating with the 5<sup>th</sup> order SMM, is that the inverse function  $U^{-1}$  is not exact. Therefore, the map we are calculating in  $w$  space, is not exactly a Hénon map. This can be improved by using higher order SMM. The bottom plot in Fig. 5 shows the frequency discrepancy improves from  $4 \times 10^{-4}$  to  $4 \times 10^{-5}$ , when 11<sup>th</sup> order SMM is used with 64 sampling points. The discrepancy further improves to  $1 \times 10^{-6}$  with 256 sampling points. However, using even larger sampling points increases the numerical noise in Fourier components and yield worse results than 256 points. It is worthwhile to note that another approach to improve the frequency accuracy is to solve the  $U^{-1}$  numerically to avoid the Taylor map truncation, which is used in this realistic example [3].

## CONCLUSION

We revisited the Hénon map by linking the nonlinear perturbed orbit to a rigid rotation by a iteration procedure. This approach follows the spirit of KAM theory. The square matrix method presents a essential tool to enable this method converge near the major resonances. The convergence of this procedure at different starting location provides a measure of the stable region in the phase space and can be used as an indicator of DA. Further studies are needed to understand the periodical motion and its relation to the dynamic aperture in higher phase space dimensions.

## REFERENCES

- [1] V. Arnold, "Small denominators, I: mappings of the circumference onto itself", *AMS Trans. Series 2*, vol. 46, pp. 213–288, 1965. doi:10.1007/978-3-642-01742-1\_10

- [2] L. Nadolski, J. Laskar, and J. Irwin, “Review of single particle dynamics for third generation light sources through frequency map analysis”, *Phys. Rev. ST Accel. Beams*, vol. 6, p. 114801, 2003. doi : 10.1103/PhysRevSTAB.6.114801
- [3] L. H. Yu, Y. Hidaka, F. Plassard, V. V. Smaluk, and Y. Hao, “Convergence Map With Action-Angle Variables Based on Square Matrix for Nonlinear Lattice Optimization”, presented at the 12th Int. Particle Accelerator Conf. (IPAC’21), Campinas, Brazil, May 2021, paper MOPAB041.